

Published in final edited form as:

*J Am Chem Soc.* 2012 February 1; 134(4): . doi:10.1021/ja211148a.

## Superhydrophobic Materials for Tunable Drug Release: Using Displacement of Air to Control Delivery Rates

Stefan T. Yohe<sup>a</sup>, Yolonda L. Colson<sup>b</sup>, and Mark W. Grinstaff<sup>a,\*</sup>

<sup>a</sup>Departments of Biomedical Engineering and Chemistry, Boston University, Boston, MA 02215.

<sup>b</sup>Division of Thoracic Surgery, Department of Surgery, Brigham and Women's Hospital, Boston, MA 02215.

### Abstract

We have prepared 3D superhydrophobic materials from biocompatible building blocks, where air acts as a barrier component in a porous electrospun mesh to control the rate at which drug is released. Specifically, we fabricated poly( $\epsilon$ -caprolactone) electrospun meshes containing poly(glycerol monostearate-co- $\epsilon$ -caprolactone) as a hydrophobic polymer dopant, which results in high apparent contact angle meshes. We demonstrate that the apparent contact angle of these meshes dictates the rate at which water penetrates into the porous network and displaces entrapped air. Addition of a model bioactive agent (SN-38) shows a release rate with a striking dependence on apparent contact angle which can be explained by this displacement of air within the electrospun meshes. We further show that porous, higher surface area electrospun meshes can be prepared to release more slowly than control non-porous constructs. Finally, the entrapped air layer within superhydrophobic meshes is shown to be robust in the presence of serum, where drug loaded meshes are efficacious against cancer cells *in vitro* for >60 days, thus demonstrating applicability for long-term drug delivery.

Superhydrophobic surfaces are characterized as those with contact angles exceeding 150°. These textured non-wetting surfaces are readily found in nature (e.g., plant leaves, and on the legs/wings of insects) and can be synthetically prepared via techniques such as templation, lithography, plasma treatment, and chemical deposition.<sup>1</sup> The phenomenon of a superhydrophobic surface is traditionally described using separate theories proposed in two landmark papers by Wenzel and Cassie. The Wenzel model characterizes a rough surface which is completely wetted in contact with a water droplet, but shows an increase in contact angle over a chemically equivalent flat surface due to surface roughness.<sup>2</sup> Alternatively, the Cassie model describes a composite surface of a hydrophobic material and air.<sup>3</sup> In this model, the energetic favorability of a water droplet to wet a high surface area hydrophobic surface is so low that air remains entrapped under the droplet, markedly increasing the apparent contact angle of the droplet. The body of superhydrophobic surface research has established that both surface roughness and surface chemistry are required to produce materials with contact angles much greater than 120°, with examples reported of surfaces with apparent contact angles as high as 160° to approaching 180°. <sup>4</sup> Given the unique property of superhydrophobicity, these surfaces are actively investigated for a variety of applications where poor wettability is favorable, including antifouling, self-cleaning, and drag reduction materials.<sup>5</sup> We hypothesized that three-dimensional (3D) superhydrophobic materials may be ideal for drug delivery applications where elution of an active agent over

\*Corresponding author mgrin@bu.edu.

SUPPORTING INFORMATION Experimental design, additional superhydrophobic mesh characterization, contact angles with serum addition. This material is available free of charge via the Internet at <http://pubs.acs.org>.

extended periods is required, since entrapped air within the material will act as a removable barrier component to slow drug release. Such a drug delivery system (DDS) is of clinical interest, for example, in pain management,<sup>6</sup> and in prevention of tumor recurrence after surgical resection.<sup>7</sup> Herein we describe the synthesis of superhydrophobic meshes from biocompatible building blocks, the characterization of the meshes by contact angle, SEM and AFM, the controlled release of an entrapped agent (SN38) as a function of material contact angle, and the efficacy of SN38 loaded meshes against a lung cancer cell line over an extended period, as well as propose a mechanism of drug release based on the Wenzel and Cassie models.

For extended drug release, we needed to create both a superhydrophobic surface and a superhydrophobic bulk material (envisioned as multiple layers or a continuum of superhydrophobic surfaces), where entrapped air acts to delay release from inner layers by slowing water penetration into the material. With this design requirement in mind, we selected the electrospinning<sup>8</sup> technique which affords textured fibers overlaid on one another to give a bulk 3D porous mesh. We chose poly( $\epsilon$ -caprolactone) (PCL) as our base polymer to electrospin since it is biocompatible and widely used in polymeric medical devices, and poly(glycerol monostearate-co- $\epsilon$ -caprolactone) (1:4) (PGC-C18)<sup>9</sup> (Fig. 1B) as a hydrophobic doping polymeric agent to be added to PCL to achieve the overall superhydrophobic state. This biocompatible copolymer of caproic acid and glycerol functionalized with stearic acid imparts a large hydrophobic effect from the stearic acid side chains.<sup>9</sup>

Specifically, PCL electrospun meshes were fabricated with varying amounts of PGC-C18 (0-50 wt%). Electrospinning processing conditions were adapted from previously published work for electrospinning PCL (Table S1).<sup>10</sup> The resulting meshes are 300  $\mu\text{m}$  thick, with an average fiber size of  $\approx 7 \mu\text{m}$ . The wettability of the meshes was assessed using static contact angle measurements as shown in Figure 2, where electrospun PCL meshes doped with PGC-C18 asymptotically approach  $153^\circ$  with 50 wt% doping. As a control material, we also prepared melted electrospun meshes by treating meshes at  $80^\circ\text{C}$  for 1 minute followed by quenching to collapse the porous structure on itself. This procedure was done quickly to prevent phase separation of PCL and PGC-C18, which was confirmed by differential scanning calorimetry (DSC) and consistent with their similar structures (Fig. S1). Studies on possible surface enrichment of the soft chain hydrophobic pendant groups of PGC-C18 are ongoing.<sup>11</sup> Electrospun meshes and melted electrospun meshes for PCL and 10% doped PGC-C18 PCL were compared using SEM and showed that the melted meshes have a comparably smooth surface (Fig. 1C-F). Additionally, the surface roughness of single electrospun fibers was quantified for PCL and PCL doped with 10% PGC-C18 using AFM. Electrospun fibers showed a finite surface roughness (RMS  $\approx 50 \text{ nm}$ ) (Fig. S2) with consistent RMS values between fibers with different PGC-C18 doping concentrations. This finite roughness indicates that both intrafiber and interfiber roughness may contribute to high apparent contact angles. The melted electrospun meshes afforded a lower maximum contact angle of  $116^\circ$  with 50 wt% doping of PGC-C18 (Fig. 2). Solvent cast films of the polymers possessed contact angles similar to the melted electrospun meshes ( $\Theta_{\text{max}}=111^\circ$ ). Surface area measurement using Kr BET on the electrospun and melted electrospun meshes showed that electrospun meshes possess at least 30X more surface area than the melted counterparts (Table S1). To further characterize the superhydrophobic character of PGC-C18 doped electrospun meshes, we performed a simple drop test to determine which meshes are in a metastable Cassie state.<sup>12</sup> We found that electrospun mesh surfaces with <25% PGC-C18 doping could be pushed into the stable Wenzel regime by dropping the water droplet used in contact angle measurements from 2 feet. Electrospun meshes with >25% PGC-C18 doping could not be pushed into the Wenzel regime in this way, suggesting that 25% doping is an approximate boundary condition for the Wenzel-to-Cassie state transition.

With the above materials prepared, we can now address our underlying hypothesis, that air entrapped within the 3D fiber mesh inhibits the penetration of water into the structure thereby slowing drug release, as drug release only occurs at the material-water interface. Moreover, as these electrospun meshes possess a high surface area compared to their melted analogs, these materials may enable us to study high surface area materials which exhibit slow drug release. We chose 7-ethyl-10-hydroxycamptothecin (SN-38) as the bioactive agent for the release studies due to its ease of detection and our previous experience.<sup>13</sup> SN-38 is the active form of the prodrug Irinotecan, an antineoplastic used in the treatment of many cancers.<sup>14</sup> Electrospun meshes and melted electrospun meshes were kept completely submerged in pH 7.4 phosphate buffered saline (PBS) during release, and release media was changed regularly to maintain sink conditions for the drug (<10% drug solubility). Figure 3 shows the release profile of porous electrospun meshes for PCL, 10% PGC-C18 doped PCL, 30% PGC-C18 doped PCL, and 50% PGC-C18 doped PCL compared to smooth melted electrospun surfaces. Electrospun PCL meshes and melted PCL meshes show similar release rates, whereas the 10% doped PGC-C18 electrospun meshes significantly slowed drug release compared to their melt control. The melted 10% PGC-C18 doped PCL meshes stop releasing SN-38 by 28 days, whereas electrospun meshes continue to release out to 70 days. The electrospun 10% PGC-C18 doped PCL mesh (i.e., the more porous and high surface area material) releases drug more slowly. These results are consistent with the observation that the 10% PGC-C18 doped PCL electrospun mesh is in the metastable-Cassie state – the material starts with air entrapped within the porous structure, and with time air is slowly displaced to create more area at the water-surface interface for SN-38 to be released. This finding provided impetus to evaluate a higher PGC-C18 doping concentration to determine if an electrospun mesh with a more stable air layer could further slow release. The 30% and 50% PGC-C18 doped electrospun meshes showed only  $\approx$ 10% SN-38 release over 9 weeks.

Next, the presence and stability of entrapped air in the meshes was confirmed via several methods. When placed in an aqueous solution, the electrospun meshes remain at the surface whereas the melted electrospun meshes sink immediately. Further, PCL meshes submerged in water for 70 days will sink independent of applied force, whereas PGC-C18 doping maintains sufficient air content over this period to prevent sinking. PCL meshes can be forced to sink with brief sonication to degas and remove the air. By increasing the PGC-C18 doping concentration to 10%, a treatment of >100-fold in sonication time is required to have the meshes sink. If 250 mL of water ( $\approx$ 1.75 kPa) is placed above a 10% PGC-C18 mesh in a filtration setup, no water passes through after 1 month while the same experimental set-up for PCL shows water penetration after 3 days. To directly visualize the water penetration in the electrospun mesh, we imaged the meshes using X-ray computed tomography in an aqueous solution containing an iodinated contrast agent (see SI). As shown in Figure 4, CT images of degassed electrospun meshes show water completely penetrated into the porous structure, whereas with native meshes only the surface has been penetrated by water (with less water at the surface of the 10% PGC-C18 doped PCL electrospun mesh), indicating that air remains within the mesh network. For comparison, melted meshes show water at the surface, consistent with the lack of porosity within the structure. Finally, an electrospun mesh that has been degassed via sonication releases its drug at a significantly faster rate. As shown in Figure 3B, 70% of the entrapped SN38 is released within 7 days from sonicated 10% doped PGC-C18 PCL electrospun meshes, compared to 70 days of release for the native electrospun mesh.

All of the above data is consistent with the release rate being dependent on the rate at which water displaces air within the electrospun meshes. The 10% PGC-C18 doped PCL electrospun mesh is in the temporary, metastable Cassie state and shows slowed release over its chemically equivalent smooth melted surface. Figure 5 presents this concept pictorially, where water penetrates into the structure in a time dependent manner to displace entrapped

air. In this way, air can act as a removable barrier component within the structure, effectively slowing drug release by controlling the rate at which the internal polymer surface area is exposed to the release media.

Next, we evaluated the SN-38-eluting electrospun meshes in a cell cytotoxicity assay where serum albumin and other biological surfactants are present. It is well established that the addition of surfactants to superhydrophobic surfaces can decrease the surface tension of water and/or adsorb to the material surface to increasing the rate of wetting<sup>15</sup>, and thus would increase the rate of drug release. To test the effect of serum on the meshes, we first performed contact angle measurements on three mesh chemistries (0, 10, 30% PGC-C18), where 10% serum was added to the applied droplet (Fig. S4). Minimal changes in contact angle were observed for all three meshes ( $< 2^\circ$ ). We next incubated electrospun meshes in 10% serum containing PBS for 24 hours to determine if longer incubation times increased protein adsorption to promote wetting. No apparent contact angle was observed for the native PCL meshes, indicating significant amounts of protein adsorption occurred to promote wetting. With the 10% and 30% PGC-C18 doped PCL meshes, only a modest decrease ( $15^\circ$  and  $4^\circ$ , respectively) in apparent contact angle was seen, showing that even in the presence of serum the entrapped air layer was present. Next, the SN-38 loaded meshes were incubated in serum containing media with Lewis Lung Carcinoma (LLC) cells (Figure 6). At a 1 wt% SN-38 concentration, both PCL and 10% PGC-C18 doped PCL meshes are cytotoxic to LLC cells for 90 days. No activity difference was seen between these meshes as even a very small amount of released SN-38 will be cytotoxic due to the low IC<sub>50</sub> of SN-38 ( $\approx 8$  ng/mL). Decreasing the SN-38 loading by 10-fold afforded a significant difference between the PCL and 10% PGC-C18 doped PCL meshes. The PCL meshes were cytotoxic for 25 days, whereas the 10% PGC-C18 doped PCL mesh was cytotoxic for 65 days. Unloaded meshes were not toxic to cells.

In summary, superhydrophobic meshes composed of hydroxycaproic acid, glycerol, and stearic acid are readily fabricated using the electrospinning technique. The resulting meshes are of high surface area and possess apparent contact angles as high as  $153^\circ$ . When the electrospun meshes are loaded with an anticancer agent (SN-38), the high apparent contact angle restricts water penetration and slows displacement of air from the high porosity meshes, thus slowing SN-38 release into the aqueous solution. The release rates of SN-38 are strikingly different when compared to the melted, nonporous analogs, as well as the degassed electrospun controls. In the presence of serum, the superhydrophobic SN-38 loaded 10% PGC-C18 doped PCL mesh is cytotoxic to LLC cells *in vitro* and performs for an extended time period. The concepts underlying our results will assist others in the preparation of new materials for drug delivery,<sup>16</sup> including translation to other polymers and drug compositions, as long as the following design specifications are maintained: 1) a material processing technique which allows production of a porous, bulk material; 2) production of constructs of sufficient thickness to promote slow, controlled water penetration; and lastly 3) a construct with a high enough apparent contact angle to entrap air within the structure and to provide a sufficient barrier for slow water penetration.

## Supplementary Material

Refer to Web version on PubMed Central for supplementary material.

## Acknowledgments

This work was supported in part by BU, CIMIT, Coulter Foundation, and NIH R01CA149561.

## REFERENCES

- (1). Li X-M, Reinhoudt D, Crego-Calama M. *Chem. Soc. Rev.* 2007; 36:1350. [PubMed: 17619692]
- (2). Wenzel RN. *J. Ind. Eng. Chem.* 1936; 28:988.
- (3). Cassie ABD, Baxter S. *T Far. Soc.* 1944; 40:546.
- (4) a). Shieh J, Hou FJ, Chen YC, Chen HM, Yang SP, Cheng CC, Chen HL. *Adv. Mater.* 2010; 22:597. [PubMed: 20217756] b) Tuteja A, Choi W, Ma M, Mabry JM, Mazzella SA, Rutledge GC, McKinley GH, Cohen RE. *Science.* 2007; 318:1618. [PubMed: 18063796]
- (5) a). Genzer J, Efimenko K. *Biofouling.* 2006; 22:339. [PubMed: 17110357] b) Nakajima A, Hashimoto K, Watanabe T. *Monatshefte fuer Chemie.* 2001; 132:31.c) Nosonovsky M, Bhushan B. *Curr. Opin. Colloid In.* 2009; 14:270.
- (6). Al Malyan M, Becchi C, Nikkola L, Viitanen P, Boncinelli S, Chiellini F, Ashammakhi N. J. *Craniofac. Surg.* 2006; 17:302. [PubMed: 16633180]
- (7). Wolinsky JB, Colson YL, Grinstaff MWJ. *Controlled Release.* 2011 (online).
- (8) a). Ma M, Hill RM, Rutledge GC. *J. Adhes. Sci. Technol.* 2008; 22:1799.b) Agarwal S, Wendorff JH, Greiner A. *Polymer.* 2008; 49:5603.c) Reneker DH, Yarin AL. *Polymer.* 2008; 49:2387.
- (9). Wolinsky JB, Ray WC III, Colson YL, Grinstaff MW. *Macromolecules.* 2007; 40:7065.
- (10). Pham QP, Sharma U, Mikos AG. *Biomacromolecules.* 2006; 7:2796. [PubMed: 17025355]
- (11) a). Yoon SC, Ratner BD. *Macromolecules.* 1986; 19:1068.b) Thomas HR, O'Malley JJ. *Macromolecules.* 1979; 12:323.
- (12). Tsai P, Pacheco S, Pirat C, Lefferts L, Lohse D. *Langmuir.* 2009; 25:12293. [PubMed: 19821629]
- (13) a). Wolinsky JB, Liu R, Walpole J, Chirieac LR, Colson YL, Grinstaff MW. *J Control Release.* 2010; 144:280. [PubMed: 20184934] b) Morgan MT, Nakanishi Y, Kroll DJ, Griset AP, Carnahan MA, Wathier M, Oberlies NH, Manikumar G, Wani MC, Grinstaff MW. *Cancer Res.* 2006; 66:11913. [PubMed: 17178889]
- (14). Mathijssen RHJ, Van Alphen RJ, Verweij J, Loos WJ, Nooter K, Stoter G, Sparreboom A. *Clin. Cancer Res.* 2001; 7:2182. [PubMed: 11489791]
- (15) a). Mohammadi R, Wassink J, Amirfazli A. *Langmuir.* 2004; 20:9657. [PubMed: 15491199] b) Ferrari M, Ravera F, Rao S, Liggieri L. *Appl. Phys. Lett.* 2006; 89:053104/1.
- (16) a). Lee CC, MacKay JA, Fréchet JM, Szoka FC. *Nat. Biotech.* 2005; 23:1517.b) Wu P, Grainger DW. *Biomaterials.* 2006; 27:2450. [PubMed: 16337266] c) Langer R, Tirrell DA. *Nature.* 2004; 428:487. [PubMed: 15057821] d) Kopecek J, Yang JY. *Polym. Int.* 2007; 56:1078.e) Hoare TR, Kohane DS. *Polymer.* 2008; 49:1993.f) Wolinsky JB, Grinstaff MW. *Adv. Drug Delivery Rev.* 2008; 60:1037.g) Davis ME, Chen Z, Shin DM. *Nature Rev. Drug Dis.* 2008; 7:771.h) Rothenfluh DA, Hubbell JA. *Integr. Biol.* 2009; 7:446.i) Kim S, Kim J-H, Jeon O, Kwon IC, Park K. *Eur. J. Pharm. Biopharm.* 2009; 71:420. [PubMed: 18977434]

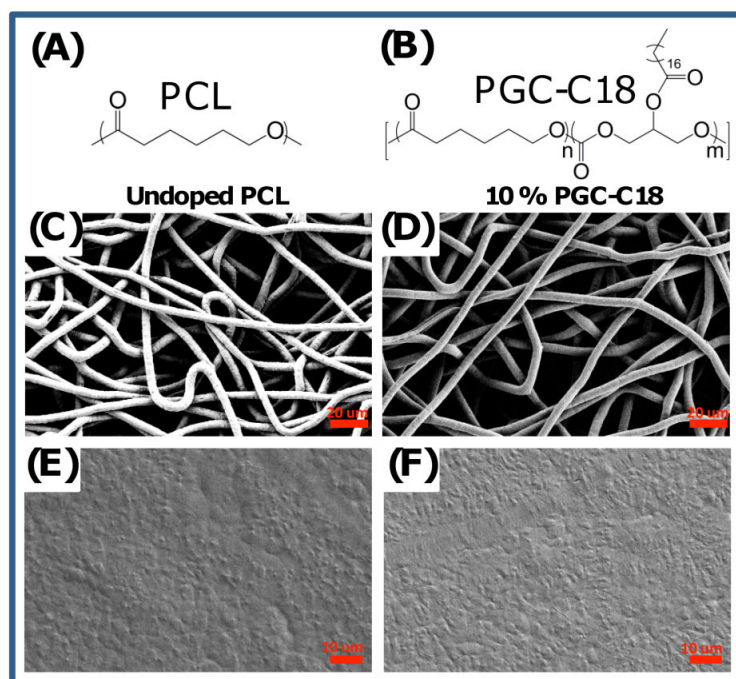


**Figure 1.**

(A) PCL was used as the base polymer for fabrication of electrospun meshes and melted electrospun meshes. (B) PGC-C18 was used as the hydrophobic dopant in PCL electrospun meshes to decrease the wettability of the meshes. (C) Electrospun PCL mesh with an average fiber size of  $7.7 \pm 1.2 \mu\text{m}$ . (D) 10% doped PGC-C18 electrospun PCL mesh with an average fiber size of  $7.2 \pm 1.4 \mu\text{m}$ . (E) A melted PCL mesh. (F) A melted 10% doped PGC-C18 electrospun PCL mesh.

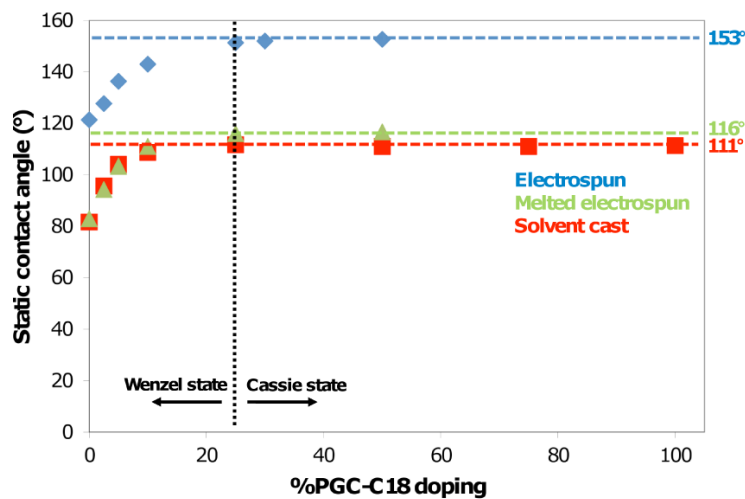


**Figure 2.** Contact angle measurements of electrospun meshes and chemically equivalent smooth surfaces as a function of PGC-C18 doping. The black dashed line indicates an approximate boundary for the Wenzel-Cassie state transition.

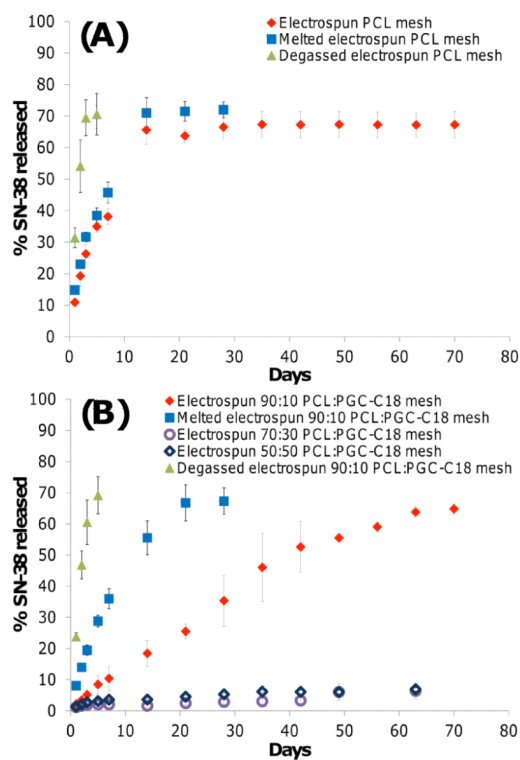


**Figure 3.** Release profiles comparing SN-38 release between (A) native, melted and degassed PCL electrospun meshes, and (B) native, melted and degassed 10% PGC-C18 doped PCL electrospun meshes as well as higher PGC-C18 doping concentration of 30 and 50 wt%.



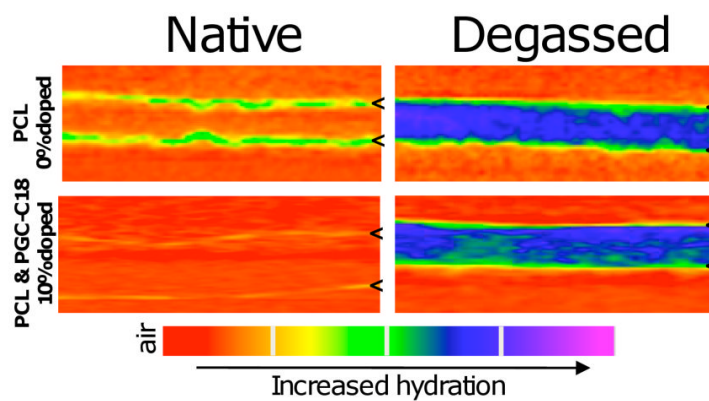


**Figure 4.** CT scans of native electrospun and degassed electrospun meshes with 0 or 10% PGC-C18 doping after incubation with the contrast agent Hexabrix for 2 hours. Degassed meshes exhibit full water penetration, while native and melted meshes (not shown) show only a low surface concentration of water. Tic marks define the top and bottom boundaries of the meshes.

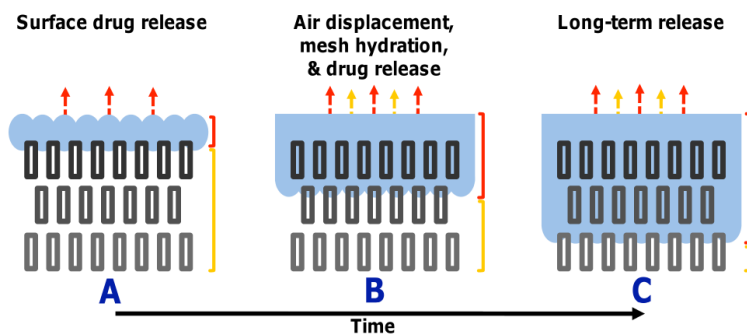


**Figure 5.** Proposed mechanism of a drug-eluting 3D superhydrophobic material in a metastable Cassie state. Over time, water slowly displaces air content from the material with the transition from the metastable Cassie state to the stable Wenzel state. If treated as iterative surfaces, water will slowly penetrate each individual surface over time enabling prolonged drug release.

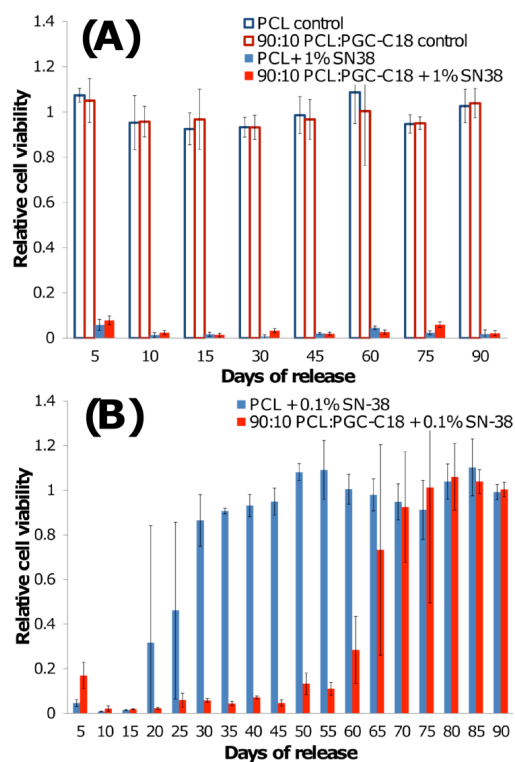


**Figure 6.** Cell cytotoxicity profiles when incubated with PCL meshes and PCL meshes with 10% PGC-C18 doping containing (A) 1 wt% or (B) 0.1 wt% SN-38. Both chemistries effectively treated LLC cells for 90 days at 1 wt% SN-38. By decreasing SN-38 concentration by 10-fold a significant difference in performance was observed, where PCL meshes were cytotoxic to LLC cells for 25 days, and the addition of 10% PGC-C18 to PCL meshes showed cytotoxicity for 65 days. Unloaded meshes were not cytotoxic to cells.